12-19-2016

Effect of disorder on the magnetic and electronic structure of a prospective spin-gapless semiconductor MnCrVAl

P. Kharel
South Dakota State University

J. Herran
University of Northern Iowa

See next page for additional authors

Effect of disorder on the magnetic and electronic structure of a prospective spin-gapless semiconductor MnCrVAl

P. Kharel,[1,2] J. Herran,[3] P. Lukashev,[4] Y. Jin,[5] J. Waybright,[1,2] S. Gilbert,[1] B. Staten,[4] P. Gray,[6] S. Valloppilly,[2] Y. Huh,[1] and D. J. Sellmyer[2,5]
[1]*Department of Physics, South Dakota State University, Brookings, South Dakota 57007, USA*
[2]*Nebraska Center for Materials and Nanoscience, University of Nebraska, Lincoln, Nebraska 68588, USA*
[3]*Department of Chemistry and Biochemistry, University of Northern Iowa, Cedar Falls, Iowa 50614, USA*
[4]*Department of Physics, University of Northern Iowa, Cedar Falls, Iowa 50614, USA*
[5]*Department of Physics and Astronomy, University of Nebraska, Lincoln, Nebraska 68588, USA*
[6]*Department of Computer Science, University of Northern Iowa, Cedar Falls, Iowa 50614, USA*

(Presented 30 November 2016; received 10 September 2016; accepted 19 September 2016; published online 19 December 2016)

Recent discovery of a new class of materials, spin-gapless semiconductors (SGS), has attracted considerable attention in the last few years, primarily due to potential applications in the emerging field of spin-based electronics (spintronics). Here, we investigate structural, electronic, and magnetic properties of one potential SGS compound, MnCrVAl, using various experimental and theoretical techniques. Our calculations show that this material exhibits ≈ 0.5 eV band gap for the majority-spin states, while for the minority-spin it is nearly gapless. The calculated magnetic moment for the completely ordered structure is 2.9 μ_B/f.u., which is different from our experimentally measured value of almost zero. This discrepancy is explained by the structural disorder. In particular, A2 type disorder, where Mn or Cr atoms exchange their positions with Al atoms, results in induced antiferromagnetic exchange coupling, which, at a certain level of disorder, effectively reduces the total magnetic moment to zero. This is consistent with our x-ray diffraction measurements which indicate the presence of A2 disorder in all of our samples. In addition, we also show that B2 disorder does not result in antiferromagnetic exchange coupling and therefore does not significantly reduce the total magnetic moment. [http://dx.doi.org/10.1063/1.4972797]

I. INTRODUCTION

Magnetic materials which are capable of producing electron current of only one spin orientation are attractive for spin transport-based devices.[1–5] Recently, a new class of materials with a semiconducting or insulating gap in one spin channel and zero gap in the other at the Fermi level, spin-gapless semiconductors, has attracted much attention because of their remarkable properties such as voltage-tunable spin polarization, the ability to switch between spin-polarized n-type and p-type conduction, high spin polarization at the Fermi level and potential high carrier mobility.[6–13] Theoretical studies have shown that several quaternary Heusler compounds including CoFeCrAl, MnCrTiSi and MnCrVAl exhibit SGS properties in their completely ordered structures.[8] However, in experiment, most of the synthesized compounds show either partial B2-type or A2-type structural disorders, which are detrimental to the spin-gapless semiconducting properties. Our interest is to synthesize MnCrVAl compound and investigate its structural and magnetic properties, and compare the experimentally observed properties with the results of first principles calculations.

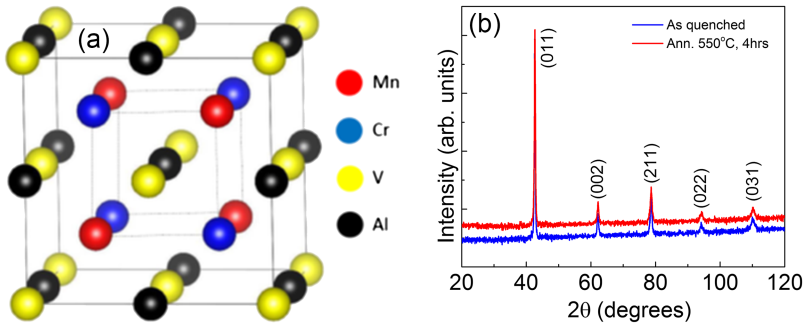

FIG. 1. (a) MnCrVAl unit cell in the completely ordered Y-structure; (b) XRD patterns of as quenched and annealed (550°C, 4 hrs) MnCrVAl powder samples.

The MnCrVAl belongs to the family of full Heusler compounds which crystallizes in a Y-structure (prototype LiMgPdSn) where V and Al occupy the Wyckoff's 4a and 4b positions, respectively, while Mn and Cr atoms alternately occupy the 4b and 4d sites, which are all located in the middle of the bcc unit cells (see Figure 1(a)). In the completely ordered Y-structure, this material is theoretically predicted to be SGS with net magnetic moment of 3.0 μ_B/f.u.[8] but there are no experimental reports to verify the theoretical predictions. Here, we report that the rapidly quenched MnCrVAl crystallizes in the A2-type disordered structure with almost zero net magnetic moment and explain with the help of first principles calculations that the cause of moment reduction is the structural disorder induced antiferromagnetic exchange coupling between displaced and non-displaced Mn and Cr atoms.

II. METHODS

A. Experimental methods

MnCrVAl compound in the form of ribbons was prepared by arc melting and rapid quenching in a melt spinner. First, MnCrVAl ingots were prepared by arc melting high-purity elements in an argon atmosphere. The ribbon samples were prepared by rapid quenching a molten mixture of MnCrVAl obtained from an induction-melting of the ingots onto the surface of a copper wheel rotating at a speed of 25 m/s. In order to find the effect of heat treatment, the ribbons were annealed at different temperatures up to 650 °C in high vacuum furnace. The experimental data presented here are from the sample annealed at 550 °C for 4 hrs, which are relatively cleaner than those of the samples annealed at other temperatures. The crystal structure of the sample was investigated using powder x-ray diffraction (XRD) in Rigaku Miniflex diffractometer with copper Kα radiation. Magnetic properties were investigated with a Quantum Design VersaLab magnetometer and Physical Properties Measurement system (PPMS). The elemental compositions of the ribbons were determined using the energy-dispersive X-ray spectroscopy (EDX) in FEI Nova NanoSEM450.

B. Computational methods

The density functional calculations of bulk Heusler compound, MnCrVAl were performed using the projector augmented-wave method (PAW),[14] implemented in the Vienna *ab initio* simulation package (VASP)[15] within the generalized-gradient approximation (GGA).[16] The integration method,[17] with a 0.05 eV width of smearing was used, along with the plane-wave cut-off energy of 500 eV and convergence criteria of 10^{-2} meV for atomic relaxation, and 10^{-3} meV for the total energy and electronic structure calculations. A *k*-point mesh of 12 × 12 × 12 was used for the Brillouin-zone integration. We used a 16-atom cubic unit cell in our calculations with the atomic arrangement shown on the Figure 1(a). Here, V and Al occupy the Wyckoff's 4a and 4b positions, respectively, while Mn and Cr atoms occupy the 4b and 4d sites, which are all located in the middle of the bcc unit cell. For all ground state calculations, unit cell geometry was fully optimized to obtain equilibrium structures and periodic boundary conditions were imposed. The effect of disorder was simulated by switching atomic positions of corresponding atoms, as explained in more details below. Some of the results were obtained using the MedeA® software environment.[18]

III. RESULTS AND DISCUSSION

A. Experimental results

Figure 1(b) shows the powder x-ray diffraction (XRD) patterns of MnCrVAl powder prepared from the ribbon samples. The XRD patterns of both the as-quenched and annealed samples contain only the fundamental peaks expected for the cubic structure of MnCrVAl. The absence of superlattice peaks (111) and (002) suggests that there is a strong A2-type atomic disorder present in the sample. Annealing the sample did not show any increase in its structural order. The diffractograms were refined with a model based on A2-type structure (Im-3m, with all the atoms sharing 2a site according to the stoichiometry) and the lattice parameter obtained is a = 2.963 Å. Diffraction data shows that the lattice parameter variation is negligibly small after the annealing process.

The isothermal magnetization curve *M(H)* measured at room temperature is shown in Fig. 2. For this measurement, a piece of ribbon sample was mounted in the VSM sample holder such that the magnetic field aligns parallel to the length of the ribbon during the measurement. As shown in the figure, the magnetization varies almost linearly with the applied magnetic field, similar to the one observed in paramagnetic or antiferromagnetic materials.[19–21] Further, the samples show very small high-field (30 kOe) magnetization, 0.3 emu/g (around 0.01 μ_B/f.u.) despite the theoretically predicted high saturation magnetization of about 3 μ_B/f.u. This large difference in saturation magnetization is attributed to the antiferromagnetic coupling between Mn and Cr atoms (in the Al sites) caused by structural disorder as discussed below.

Fig. 3 shows the thermomagnetic curve *M(T)* of the 550 °C-annealed MnCrVAl ribbon measured at 5 kOe between 50 K and 900 K. As shown in the figure, the magnetization first increases monotonically with increasing temperature above 50 K and passes through a magnetic anomaly at 560 K, although the magnetization shows a weak dependence on temperature. This anomaly may represent a magnetic transition from an antiferromagnetic to a paramagnetic phase.[21–23] Similar magnetic transition has been observed in another disordered compound Mn_3Ga.[24] Khmelevskyi *et al.* predicted from first principles calculations that this anomaly is the consequence of a strong antiferromagnetic nearest-neighbor coupling in the disordered Mn_3Ga.[25] Although our MnCrVAl ribbons have a disordered structure, this anomaly at 560 K is not consistent with the regular spin glass transition because magnetizations between the zero-field-cooled (ZFC) and field-cooled (FC) measurements are totally reversible.

B. Computational results

In order to investigate the ground state properties of MnCrVAl and elucidate the experimentally observed results, we have performed density functional calculations of the completely ordered (Y-type structure) and partially disordered (both B2 and A2 type) bulk MnCrVAl compound. We first calculated the equilibrium lattice constant by minimizing energy per unit cell. As shown in Fig. 4,

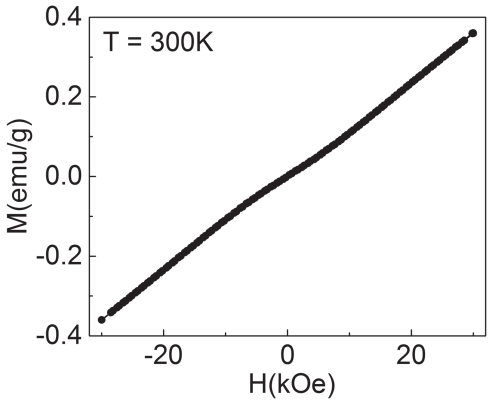

FIG. 2. The room-temperature magnetization M, as a function of magnetic field H of the 550 °C-annealed MnCrVAl ribbon.

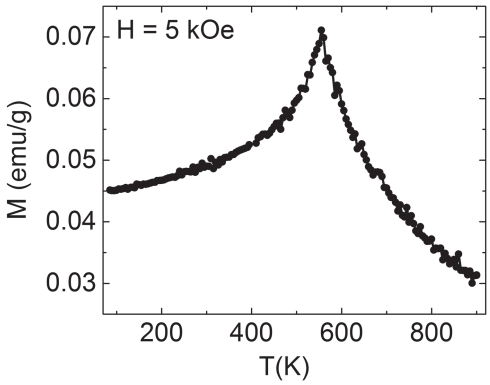

FIG. 3. The magnetization M, as a function of temperature T of the 550°C-annealed MnCrVAl ribbon measured at 5 kOe.

the equilibrium lattice constant a for the completely ordered (Y-structured) unit cell of MnCrVAl is 5.903 Å close to the value obtained from XRD analysis.

Figure 5 shows the site-projected densities of states (DOS) of cubic MnCrVAl in the ground state. The majority-spin DOS is essentially zero at the Fermi level (the very small contribution from Mn and Cr is probably the computational artefact, such as the width of smearing) with band gap of ≈ 0.5 eV. Further, the minority-spin DOS demonstrates almost gapless semiconducting behavior consistent with the previous report.[8] The minority-spin valence band maximum is almost entirely formed by the Mn states, while the minimum of the unoccupied minority-states has comparable contribution from Mn, Cr, and V.

The total calculated magnetic moment for 16 atom MnCrVAl cell is m_{total} =11.60 μ_B (2.9 μ_B/f.u.), where the atom resolved moments are 1.79 μ_B, 2.08 μ_B, -0.96 μ_B and -0.01 μ_B per four atoms of Mn, Cr, V and Al, respectively. This value of total magnetization does not agree with our experimentally measured value, which motivated us to further investigate the disordered structures as suggested by XRD results. In order to find the effect of disorder on the magnetic properties of MnCrVAl, we performed series of calculations for various disorder combinations, by exchanging atomic positions of Mn-Al, Cr-Al, and V-Al pairs (the first two combinations are usually referred to as A2 disorder, while V-Al exchange is B2 disorder). In all considered cases the crystal structure was fully optimized, by minimizing energy. Our calculations show that the B2-type disorder does not produce significant change in the total magnetic moment. In this case, the total magnetic moment per 16-atom cell lies between 11 μ_B and 11.5 μ_B based on the positions being changed. On the other hand, the A2-type disorder was found to produce significant reduction of the total magnetic moment of MnCrVAl. We found that the mangetic moment per 16-atom cell decreases by a factor of two (m_{total} = 5.92 μ_B) when one Mn or one Cr atom exchange positions with Al. At the same time, exchanging the positions of

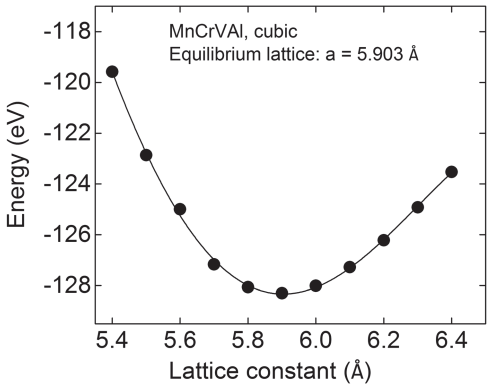

FIG. 4. Energy versus lattice constant of bulk cubic MnCrVAl.

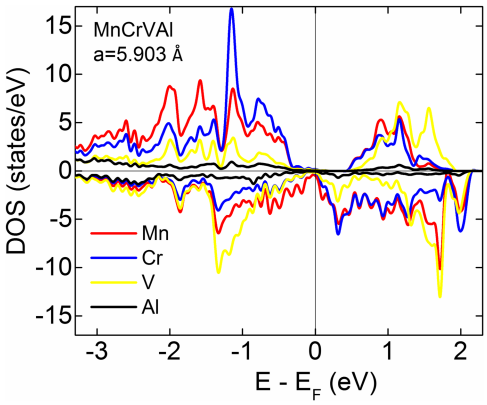

FIG. 5. Atom-resolved densities of states of the bulk cubic MnCrVAl. Atomic contributions are color coded as indicated on the figure.

two Mn (or two Cr) atoms with two Al atoms results in almost zero total magnetic moment consistent with our experimental data.

Our calculations suggest that the disorder-induced magnetization reduction in MnCrVAl is mainly due to the antiferromagnetic exchange coupling between displaced (i.e., the atoms occupying Al sites) and non-displaced Mn and Cr atoms. For example, after exchanging positions of one Mn atom with Al, the calculated magnetic moment of the displaced Mn atom becomes -2.34 μ_B, while the magnetic moments per non-displaced Cr atom decreases from 2.08 μ_B to 1.68 μ_B. If two Mn (or Cr) atoms exchange positions with two Al atoms, the magnetic moments of the displaced atoms are opposite to the magnetic moments of regular-site Mn and Cr atoms, resulting in the zero net magnetic moment. The disorder induced modification of magnetic structure is probably due to the change in the crystal field of the displaced atoms.

IV. CONCLUSIONS

Results of combined experimental and theoretical study of structural, electronic, and magnetic properties of potential spin-gapless semiconductor, MnCrVAl are presented. It is shown that this material exhibits nearly spin-gapless semiconducting behavior in fully ordered crystal structure. Further, our XRD measurements indicate that A2-type structural disorder (exchange of Mn/Cr and Al atomic positions) is present in all of our samples. First principles calculations indicate that this disorder results in induced antiferromagnetic exchange coupling between displaced and regular-site Mn and Cr atoms, which effectively reduces the total magnetic moment of this material to zero. The disorder induced antiferromagnetic coupling is probably due to the modified crystal field. These interesting results add to the growing literature on the effect of disorder on the properties of potential spin-gapless semiconductors.

ACKNOWLEDGMENTS

This research is supported by Research/Scholarship Support Fund, SDSU. Research at UNI is supported by the Pre-Tenure Grant from the Office of the Provost and Executive Vice President for Academic Affairs, UNI, as well as from the UNI Faculty Summer Fellowship. Computations were performed at the University of Northern Iowa computer cluster. Research at UNL is supported by US DOE (DE-FG02-04ER46152, NSF-DMR under Award DMREF: SusChEM 1436385. The work was performed in part in the Nebraska Nanoscale Facility, Nebraska Center for Materials and Nanoscience, which is supported by the National Science Foundation under Award ECCS: 1542182, and the Nebraska Research Initiative.

[1] E. E. Y. Tsymbal and I. Žutić, *Handbook of Spin Transport and Magnetism* (CRC press, Boca Raton, FL, 2011), 808 pp.
[2] R. A. de Groot, F. M. Mueller, P. G. v. Engen, and K. H. J. Buschow, Physical Review Letters **50**(25), 2024–2027 (1983).
[3] I. H. A. I. Galanakis, in *Springer Series in Materials Science 222*, edited by C. Felser and A. Hirohata (Springer International Publishing Switzerland, 2016).

[4] E. Şaşıoğlu, L. M. Sandratskii, P. Bruno, and I. Galanakis, Physical Review B **72**(18), 184415 (2005).
[5] G. H. F. B. Balke, J. Winterlik, and C. Felser, Appl. Phys. Lett. **90**, 152504 (2007).
[6] X. L. Wang, Physical Review Letters **100**(15), 156404 (2008).
[7] S. Ouardi, G. H. Fecher, C. Felser, and J. Kübler, Physical Review Letters **110**(10), 100401 (2013).
[8] K. Özdoğan, E. Şaşıoğlu, and I. Galanakis, Journal of Applied Physics **113**(19), 193903 (2013).
[9] A. Nelson, Y. Huh, P. Kharel, V. R. Shah, R. Skomski, and D. J. Sellmyer, Journal of Applied Physics **115**(17), 17A923 (2014).
[10] P. Lukashev, P. Kharel, S. Gilbert, B. Staten, N. Hurley, R. Fuglsby, Y. Huh, S. Valloppilly, W. Zhang, K. Yang, R. Skomski, and D. J. Sellmyer, Applied Physics Letters **108**(14), 141901 (2016).
[11] H. Ohno, Nat Mater **9**(12), 952–954 (2010).
[12] P. K. R. P. Panguluri, C. Sudakar, R. Naik, R. Suryanarayan, V. M. Naik, A. G. Petukhov, B. Nadgorny, and G. Lawes, Phys. Rev. B **79**, 165208 (2009).
[13] Y. Jin, P. Kharel, P. Lukashev, S. Valloppilly, B. Staten, J. Herran, I. Tutic, M. Mitrakumar, B. Bhusal, A. Connell, K. Yang, Y. Huh, R. Skomski, and D. J. Sellmyer, Journal of Applied Physics **120**(5), 053903 (2016).
[14] P. E. Blöchl, Physical Review B **50**(24), 17953–17979 (1994).
[15] G. Kresse and D. Joubert, Physical Review B **59**(3), 1758–1775 (1999).
[16] J. P. Perdew, K. Burke, and M. Ernzerhof, Physical Review Letters **77**(18), 3865–3868 (1996).
[17] M. Methfessel and A. T. Paxton, Physical Review B **40**(6), 3616–3621 (1989).
[18] (MedeA® Version 2.19. MedeA® is a registered trademark of Materials Design, Inc. Angel Fire, New Mexico, USA.)
[19] X. Wang, M. Zhu, L. K. Koopal, W. Li, W. Xu, F. Liu, J. Zhang, Q. Liu, X. Feng, and D. L. Sparks, Environmental Science: Nano **3**(1), 190–202 (2016).
[20] S. Nakatsuji, N. Kiyohara, and T. Higo, Nature **527**(7577), 212-215 (2015).
[21] L. Wang, Y. G. Cui, J. F. Wan, J. H. Zhang, and Y. H. Rong, AIP Advances **3**(8), 082126 (2013).
[22] R.-G. Cai and R.-Q. Yang, Physical Review D **91**(8), 086001 (2015).
[23] J. F. Niven, M. B. Johnson, A. Bourque, P. J. Murray, D. D. James, H. A. Dąbkowska, B. D. Gaulin, and M. A. White, Proceedings of the Royal Society A: Mathematical, Physical and Engineering Science **470**(2171) (2014).
[24] P. Kharel, Y. Huh, N. Al-Aqtash, V. R. Shah, R. F. Sabirianov, R. Skomski, and D. J. Sellmyer, Journal of Physics: Condensed Matter **26**(12), 126001 (2014).
[25] S. Khmelevskyi, A. V. Ruban, and P. Mohn, Physical Review B **93**(18), 184404 (2016).